Journal of Controlled Release 142 (2010) 474–482

Contents lists available at ScienceDirect

Journal of Controlled Release

journal homepage: www.elsevier.com/locate/jconrel

Parameter estimation methodology in a model of hydrophobic drug release from a polymer coating

Rachael W. Sirianni [a], Eun-Hyun Jang [b], Kathleen M. Miller [b], W. Mark Saltzman [a,*]

[a] Dept. of Biomedical Engineering, Yale University, 55 Prospect St., New Haven, CT 06511, USA
[b] Boston Scientific Corporation Inc., 1 Boston Scientific Place, Natick, MA 01760, USA

ARTICLE INFO

Article history:
Received 18 September 2009
Accepted 22 November 2009
Available online 1 December 2009

Keywords:
Mathematical model
Paclitaxel
Hydrophobic
Controlled release
Polymer

ABSTRACT

The TAXUS® Express® coronary artery stent delivers a sustained dose of a hydrophobic drug (paclitaxel) from a hydrophobic polymer coating (poly(styrene–isobutylene–styrene), SIBS). It is known that particles of concentrated drug are dispersed throughout the polymer coating, however, the mechanism by which drug exits the polymer matrix is not fully characterized. In this work, mathematical models were applied to *in vitro* controlled release data obtained from 8.8, 25 and 35% loadings of drug in polymer. Models that accounted for release by different mechanisms were tested. It was observed that Fickian diffusion, dissolution and osmotic gradient models were capable of fitting the data equally well. It was also possible to fit the data with a variety of parameter combinations, even if the values of some parameters were unlikely. We use the example of Paclitaxel release from the SIBS matrix to discuss important considerations in fitting controlled release data with mechanistic models.

1. Introduction

Paclitaxel (PTx) is a 0.96 kDa, hydrophobic molecule that was originally extracted from the inner bark of the Pacific Yew Tree. PTx is a potent anti-proliferative agent that halts the mitotic process by binding to microtubules in cells [1]. The anti-proliferative activity of PTx led to its historic success as an anticancer agent and, in recent years, to the application of PTx in the treatment of coronary artery restenosis. The combination of PTx with a coronary vascular stent as a component of a local drug delivery matrix has expanded the field of interventional cardiology [2].

The TAXUS® Express® coronary stent (Boston Scientific Corporation) is a drug-eluting coronary artery stent that slowly delivers PTx to the vascular wall (Fig. 1). Release of PTx from the polymer coating on the stent surface reduces the process of neointimal hyperplasia in the vascular wall, resulting in a drug eluting stent that has greater long term efficacy than traditional bare metal stents [3]. Between 2002 and 2008, nearly five million TAXUS stents were implanted in over 3.4 million patients, demonstrating clinical success in reducing stent-related restenosis. Although the TAXUS® family of drug eluting stents have proven long term safety and efficacy profiles, the understanding of the underlying complex physicochemical mechanisms that control drug release from the stent coating is limited. The focus of the studies presented here is to expand that understanding.

The TAXUS® Express® stent is constructed by a solvent evaporation method whereby a dissolved coating consisting of poly(styrene–isobutylene–styrene) (SIBS) and PTx is applied to a stainless steel bare metal stent. Solid-state NMR, thermal and atomic force microscopy (AFM) experiments suggest that PTx is not miscible in SIBS [4,5], and water does not significantly absorb into SIBS (personal communication, Boston Scientific Corporation). Yet, under certain formulation conditions, slow release of drug from SIBS polymer has been observed over long time frames. Since PTx is only sparingly soluble in water, it is not clear how drug exits the polymer matrix.

Mathematical models have been an important tool in the development of controlled release systems for several decades. For example, the now-classic Higuchi model still provides a valuable point of reference for the analysis of many delivery systems [6,7]. Ideally, a mathematical model of a controlled release system would be constructed from general governing equations and would provide reliable predictions of drug release rates as a function of polymer composition. A variety of models have been developed to describe the release of drug from a polymer matrix based on primary mechanisms of drug release, such as degradation, swelling or erosion; all of these processes are diffusive in nature [8–12]. Alternative, non-diffusive mechanisms of drug release have also been proposed for various applications [13–16]. Investigators often attempt to use a mathematical model to identify physical mechanisms underlying the release of drugs from polymer materials [17–20], but the comparison of models based on different mechanisms is a less common practice [7,21–23].

* Corresponding author. Tel.: +1 203 432 4262; fax: +1 203 432 0030.
E-mail address: mark.saltzman@yale.edu (W.M. Saltzman).

0168-3659/$ – see front matter © 2009 Elsevier B.V. All rights reserved.
doi:10.1016/j.jconrel.2009.11.021

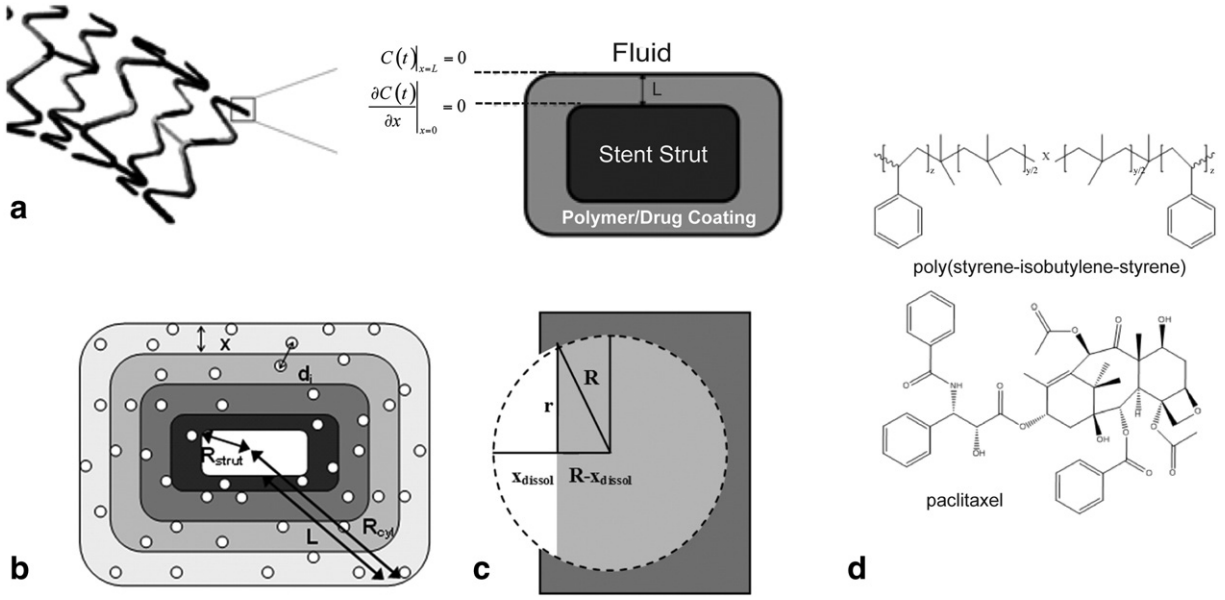

Fig. 1. Schematic of drug release from the polymer coating on the TAXUS® Express® stent. (a) In the diffusion and diffusion with bulk dissolution models, drug diffuses from the polymer phase to the fluid phase. The flux is zero at the stent-strut interface, such that $\partial C/\partial x|_{x=0}=0$, and sink conditions are maintained at the polymer-fluid interface, such that $C(x=L)=0$. (b) In the osmotic gradient model, a metal strut of radius R_{strut} is coated with polymer containing drug. The polymer coating is of thickness L, yielding a total cylinder radius of $R_{cyl}=R_{strut}+L$. Individual drug particle centers are separated by d_i. The cross section of the cylinder is divided into concentric annuli of width x, the average distance between particle centers, which is a function of loading percent and average particle radius. (c) In the surface dissolution model, a moving front of fluid dissolves particles of drug with convective transfer coefficient, h. The exposed particle surface area (πr^2) is a function of dissolution depth (x_{dissol}) and time (t). (d) Chemical structures of poly(styrene–isobutylene–styrene) (SIBS) and paclitaxel (PTx).

Comparison of multiple controlled release models could increase confidence in the identification of release mechanisms.

In this work, multiple mathematical models were examined with the goal of testing hypotheses regarding the mechanism of hydrophobic drug release from the polymer film. The quantitative results reported here specifically pertain to the release of paclitaxel from the TAXUS® Express® coronary stent, however, we are also concerned with the more general case of fitting controlled release data with mechanistic models. We will also discuss potential shortcomings of data fitting methods that are typical in the field of drug delivery.

2. Methods

2.1. Controlled release measurement

The release kinetics of paclitaxel were characterized *in vitro* by incubating individual stents in 1.5 mL (slow release formulations, $n=3$) or 15.0 mL (moderate and fast release formulations, $n=12$ and $n=4$, respectively) of medium at 37 °C and pH 7.4. The incubation medium consisted of 0.01 M phosphate buffered saline containing 0.05% Tween 20 (PBS-Tween20, Sigma, St. Louis, MO). Tween 20 was added to the media in order to prevent non-specific adsorption of PTx to glass and plastic surfaces; this formulation has been demonstrated to have a 1:1 correlation with *in vivo* release studies (data not shown). Furthermore, the data collected here are representative of numerous studies conducted over several years. At selected time points, medium was completely removed from incubation vials for analysis and replaced with fresh medium to maintain sink conditions. PTx concentrations were determined by HPLC. Chromatography was performed using a Waters Alliance 2695 Separation Module with 2996 Photodiode Array (PDA) detector. The separation was accomplished using an Waters Symmetry C18 reversed-phase column (4.6 mm ID × 75 mm, 3.5 µm) maintained at 30 °C with isocratic elution using Acetonitrile/20 mM SDS + Sodium Monobasic Phosphate (1:1) at flow rate of 1.0 mL/min, with a detection wavelength of 227 nm.

2.2. Atomic force microscopy

Sub-surface morphologies of the polymer-drug stent coatings were examined by AFM on samples prepared by a cryogenic microtomy technique. Cryomicrotomy was performed using a Leica Ultracut UCT main unit, a Leica EM FCS cryo unit and a Diatome Cryo-Ultra 35° diamond blade. Stents were mounted and secured on stainless steel rods and angled for blade access. A Multi-Mode AFM (Digital Instruments/Veeco Metrology, Santa Barbara, CA) was controlled with NanoScope IIIa and NanoScope Extender electronics to obtain the AFM images. For ultrathin sub-surface samples, measurements were made using TappingMode AFM in air, a technique that is usually less perturbing to soft samples than Contact Mode AFM. The AFM probe was a Tap300 Metrology Probes (NanoDevices, Santa Barbara, CA). Scan rate, drive amplitude, feedback setpoint and gain parameters were optimized so that the AFM probe was able to track the stent surface at high resolution and low noise. Phase imaging, which can lead to simultaneous acquisition of phase (material property) information as well as topography (texture) of the material, was used to capture image data. AFM analysis of ultrathin subsurface sections was performed at BIOMETROLOGY, Inc. (Alameda, CA), and the ultrathin cryo sections were prepared in conjunction with nanoAnalytics (Münster, Germany).

2.3. Mathematical model: diffusion

Fick's Law can be used to describe diffusion of drug through a polymer material, where the rate of diffusion over elapsed time (t) is assumed to be directly proportional to the concentration gradient of drug in the polymer coating (C_p). For diffusion in a single dimension (x), Fick's Law takes the following form:

$$\frac{\partial C_p}{\partial t} = D\frac{\partial^2 C_p}{\partial x^2} \tag{1}$$

Fick's Law can also be used to estimate the diffusion coefficient, D, from experimental data. The diffusion coefficient is empirically

determined by fitting solutions to Eq. (1) to data that are collected under conditions in which the equation is valid. To apply Eq. (1) directly, the system under study must be homogeneous across a finite distance under consideration. For systems that are not homogeneous with respect to diffusion (in porous structures, for example, permeable and impermeable regions distribute through a network of interconnecting pores), Eq. (1) can sometimes still be used, but D is interpreted as an effective diffusion coefficient, D_{eff}.

The following assumptions were made to use Eq. (1) to describe release from stent coatings *in vitro* (Fig. 1a): (1) uniform distribution of drug throughout the polymer coating, (2) zero concentration of drug at the polymer/fluid interface ($x=L$) at all times (sink conditions in fluid), (3) zero flux at polymer/strut interface ($x=0$) at all times, (4) isotropic material properties, and (5) homogeneous distribution of drug through polymer of total thickness L. This system was solved numerically by using a built-in partial differential equation solver function in Matlab v7.1. Numerical analysis resulted in a prediction of drug concentration in the polymer phase, C, as a function of t and x for a given value of D. Since the total loading of drug in polymer is ϕ, the final expression for cumulative fractional release of drug to the fluid phase is given by:

$$C_b = 1-\frac{1}{\phi}\int C_p \cdot dx \tag{2}$$

2.4. Mathematical model: bulk dissolution

The analysis described above for pure Fickian diffusion of drug through polymer relies on the assumption that the drug is dissolved homogeneously throughout the polymer matrix. This assumption implies that any drug contained in the polymer coating is immediately mobile and available for release via diffusion. Previous physical analysis suggest that this is unlikely to be true for the TAXUS® Express® stent [4]: it is known that drug rich and polymer rich phases exist in the same region of interest. Therefore, it is anticipated that PTx must dissolve from the drug phase into the polymer phase prior to transport via diffusive mechanisms. To account for this additional transport mechanism, a source term for bulk dissolution was derived from a mass balance that assumes flux from a drug particle is related to its surface area (spherical drug particles of radius R), the transfer coefficient from drug to polymer (k), and the difference between the concentration of drug dissolved in polymer, C_p, and its saturation level, C_{sat}:

$$source\,term = \frac{particle}{volume}\times\frac{flux}{particle} = \left(\frac{C_0}{4/3\pi\cdot R^3}\right)\times\left[4\pi\cdot R^2\cdot k(C_{sat}-C_p)\right] \tag{3}$$

The source term describes flux from drug to polymer for a given differential volume (notice that C_p, C_0 and C_{sat} are expressed in units of weight fraction). The particulate source of drug is only considered to contribute to $\partial C_p/\partial t$ when the drug concentration is greater than C_{sat}. When the concentration of drug falls below saturation, release proceeds via the diffusion process only. This expression is incorporated into the differential equation for bulk diffusion through the polymer phase:

$$\frac{\partial C_p}{\partial t} = \begin{cases} D\dfrac{\partial^2 C_p}{\partial x^2}-3C_0\dfrac{k}{R}(C_p-C_{sat}) & \text{for } C_p\geq C_{sat} \\ D\dfrac{\partial^2 C_p}{\partial x^2} & \text{for } C_p<C_{sat} \end{cases} \tag{4}$$

Eq. (4) does not have a straightforward analytical solution and therefore must be evaluated numerically, using the boundary conditions described in Fig. 1a and methods Section 2.3. Summing the concentration across the polymer coating yields the percent cumulative release due to combined bulk diffusion and dissolution (Eq. (2)).

2.5. Mathematical model: osmotic gradient

Controlled release data collected for the TAXUS® Express® stent revealed that after an initial high rate of release, the rate of release is relatively constant for a sustained period of time. This relatively constant rate of release for a sustained period of time is a feature not expected based on diffusion-mediated release. To the best of our knowledge, there are no existing models of drug release that would provide a likely mechanism for the release of paclitaxel from the TAXUS® Express® stent. To explore alternate mechanisms for drug release, we examined a model previously developed for hydrophilic drugs in hydrophobic materials [16]. We were aware that paclitaxel is not a hydrophilic drug (in fact, it is quite hydrophobic), but we believed that this alternate was still an interesting model to use for comparison, since it predicts the near zero-order release observed for the commercial TAXUS® Express® stent formulation. For the osmotic gradient model, a multiphase material structure is assumed, where spherical particles are drug rich and the surrounding hydrophobic material is assumed to be impermeable to both solvent and drug. The drug phase forms so-called 'capsules', where each capsule is separated from the next capsule by the distance d_i. As solvent fills a capsule, osmotic pressure builds to the point of bursting, thus forming a channel to the next capsule and creating a network for solvent to diffuse in and drug to diffuse out of the polymer (Fig. 1b).

The release profile generated by this osmotic gradient model depends on the geometry of the system of interest. Release occurs from the outermost layers inward, with swelling capsules occurring within an annulus of active swelling whose radial position moves inward with time. Although drug release occurs in a continuous manner (i.e., not stepwise), only those capsules within the annulus' width are swollen with solvent and therefore bursting at any particular time. To calculate x, which is the average of individual d_i, as a function of particle radius, the volume of the stent coating is divided by the number of particles. Each unit volume contains one particle of radius R and is of length/width/height x. The volume of an individual cube times the loading of drug in polymer is equal to the volume of a particle of drug. Solving for x yields the following expression:

$$x = \left(\frac{4\pi}{3\phi}\right)^{1/3}R \tag{5}$$

Thus, x defines the system by determining the typical distance between particles that are in the process of swelling at any given time based on the overall loading of drug in polymer. Details of the model derivation are described by Amsden [16]. The resulting equation for release as a function of time depends on the radius of the stent (R_{cyl}), width of an annulus (x), and the time for a capsule to burst (t_b, an empirically determined parameter):

$$C_{cyl} = \frac{1}{1+R_{cyl}/x}\left[\left(2+\frac{x}{R_{cyl}}\right)\left(\frac{t}{t_b}\right)-\frac{x}{R_{cyl}}\left(\frac{t}{t_b}\right)^2\right] \tag{6}$$

For this application, a polymer coating is applied to a stainless steel strut; the strut has a rectangular cross section, however, the polymer is curved across the corners of the strut. The geometry of the system is therefore not purely cylindrical or purely rectangular. From our simulations (data not shown), there is negligible ($\leq$1%) difference in the cumulative release predicted by Fickian diffusion for cylindrical versus rectangular geometry. The issue of planar versus cylindrical geometry is different for the osmotic gradient model. For the osmotic gradient model, the release rate is constant at all stages of release in rectangular coordinates, whereas it is observed to speed up at later stages of release in cylindrical coordinates. The acceleration in release rate is due to a reduction in the volume of each concentric annulus as

release reaches the interior of the polymer. For the osmotic gradient model, the curvature present at each of the corners of the polymer coating has a significant influence on release. We therefore adapted the osmotic gradient model to be "semi-cylindrical" by accounting for how the radius of curvature affects the volume of polymer available for drug release. The radius of curvature for the polymer coating, R_{cyl}, is given by the radius of the strut, R_{strut}, plus the coating thickness, L:

$$R_{cyl} = R_{strut} + L \tag{7}$$

The fraction of the volume that corresponds to the polymer coating is expressed by $f_{critical}$:

$$f_{critical} = \frac{\pi R_{cyl}^2 L - \pi R_{strut}^2 L}{\pi R_{cyl}^2 L} = 1 - \frac{R_{strut}^2}{R_{cyl}^2} \tag{8}$$

Eq. (6) is therefore modified to express the correct cumulative release fraction:

$$C_b = \frac{1}{f_{critical}} \cdot \begin{cases} \frac{1}{1 + R_{cyl}/x}\left[\left(1 + \frac{x}{R_{cyl}}\right)\left(\frac{t}{t_b}\right) - \left(\frac{x}{R_{cyl}}\right)\left(\frac{t}{t_b}\right)^2\right] & \text{for } C_{cyl} \le f_{critical} \\ f_{critical} & \text{for } C_{cyl} > f_{critical} \end{cases} \tag{9}$$

2.6. Mathematical model: surface dissolution

Particles of drug that touch the fluid surface release faster than drug distributed through the bulk polymer. Drug released via surface dissolution is a likely mechanism to account for the more rapid release rate that is observed at early time points for most controlled release systems. Surface dissolution can be described through a mass balance that considers particles touching the surface, where the flux (J) is related to the surface of particle exposed, the mass transfer coefficient of drug to media (h), and solubility of drug in media (C_m). For a single particle (Fig. 1c):

$$J \cdot dt = \pi \cdot r(t)^2 \cdot h C_m dt \tag{10}$$

Note that r is the exposed particle radius as a function of time whereas R is the fixed radius. The flux equation is also related to the mass of drug in a differential depth with density ρ:

$$J \cdot dt = \pi \cdot r(t)^2 \cdot \rho \cdot dx_{dissol} \tag{11}$$

Yielding a relationship between the dissolution depth (x_{dissol}) and time:

$$x_{dissol} = \frac{h \cdot C_m}{\rho} \cdot t \tag{12}$$

The exposed particle radius as a function of time is defined in terms of dissolution depth and particle radius R:

$$r(t)^2 = [R^2 - (R - x_{dissol})^2] = 2R \cdot x_{dissol} - x_{dissol}^2 \tag{13}$$

The particle volume is also a function of time, $V(t)$, given by:

$$V(t) = \int \pi \cdot r(t)^2 dx_{dissol} \tag{14}$$

Table 1
Various models of drug release with schematics.

Mechanism	Schematic	Governing equation	Conditions
Diffusion[a]	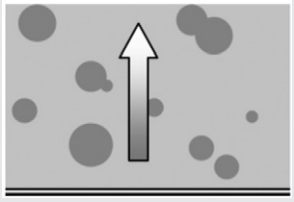	$\frac{\partial C}{\partial t} = D\frac{\partial^2 C}{\partial x^2}$	Drug must be mobile within polymer phase
Diffusion with bulk dissolution[a]	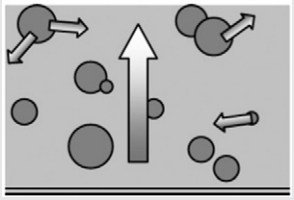	$\frac{\partial C}{\partial t} = D\frac{\partial^2 C_b}{\partial x^2} - 3C_0\frac{k}{R}(C - C_{sat})$	The concentration of drug be above its solubility limit in polymer; drug must dissolve into polymer phase prior to a availability for diffusion
Osmotic gradient	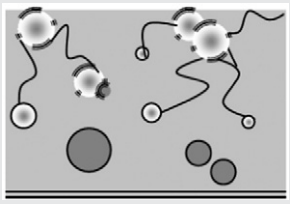	$C_b = \frac{1}{1 + R_{cyl}/x}\left[\left(2 + \frac{x}{R_{cyl}}\right)\left(\frac{t}{t_b}\right) - \frac{x}{R_{cyl}}\left(\frac{t}{t_b}\right)^2\right]$	Polymer must be impermeable to water; drug must possess some osmotic activity
Surface dissolution	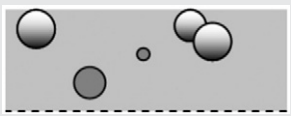	$C_s = \frac{3}{4}\left((\omega \cdot t)^2 - \frac{1}{3}(\omega \cdot t)^3\right)$	Particles touching the surface of the polymer must be available for release via convective mechanisms

[a] Cumulative release of drug is given by $C_b = 1 - \frac{1}{\phi}\int C(t,x)dx$.

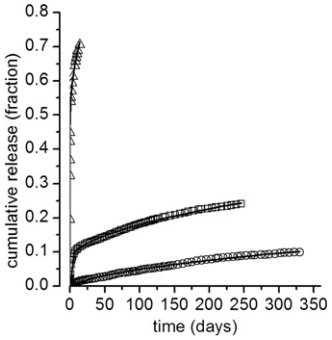

Fig. 2. Predicting the release of PTx from SIBS with Fick's Law. The experimentally measured release of PTx from SIBS (○ 8.8, □ 25 and △ 35% loading of drug in polymer) matched well with predictions of drug release based on Fickian diffusion with surface dissolution. Data fits were obtained with diffusion coefficients (D) of 5.2, 2.2 and 110×10^{-10} m^2/s, surface release fractions, ζ, of 0.005, 0.09 and 0.5, and ω of 6, 3 and 80×10^{-6} s^{-1} for 8.8, 25 and 35% loading, respectively.

Combining Eqs. (12) and (13) and integrating over the volume in Eq. (14) yields an expression for the volume of particle released as a function of time:

$$V(t) = \pi\cdot R\cdot\left(\frac{hC_m}{\rho}\right)^2\left[t^2-\left(\frac{hC_m}{3\rho}\right)t^3\right] \tag{15}$$

Dividing by the total volume of a particle yields an expression for the percent cumulative release due to surface dissolution:

$$C_s = \frac{3}{4}\left[\left(\frac{hC_m}{\rho R}\right)^2 t^2-\frac{1}{3}\left(\frac{hC_m}{\rho R}\right)^3 t^3\right] \tag{16}$$

The mathematical symmetry of this equation is useful. Notice that, by defining a new parameter, ω:

$$\omega = \frac{hC_m}{\rho R} \tag{17}$$

we obtain a compact expression for the fractional release from surface drug:

$$C_s = \frac{3}{4}\left((\omega\cdot t)^2-\frac{1}{3}(\omega\cdot t)^3\right) \tag{18}$$

Eqs. (15)–(18) apply for the duration of surface release, i.e., $0\le t\le 2/\omega$.

2.7. Summary of models and parameters

A summary of the mathematical expressions developed for this work – as well as schematics describing the associated release mechanisms – are provided in Table 1. Eqs. (1), (4), and (9) are models that describe primary mechanisms of drug release from the polymer network, whereas Eq. (18) is a description of release from the surface only, and thus can be added to any of the above three models. The relative contribution of the surface dissolution model depends on the percentage of particles (ζ) that are assumed to touch the fluid interface. If homogeneous distribution throughout the stent coating is assumed, then ζ is simply given by R/L. For this analysis, Eqs. (1), (4) and (9) were each examined independently and then considered with the addition of the surface dissolution described above. The expression for cumulative release of drug from the bulk polymer phase with surface dissolution is given by:

$$C_{total} = \begin{Bmatrix} \zeta\cdot C_s + (1-\zeta)\cdot C_b & \text{for} & t\le t_{surf} \\ \zeta + (1-\zeta)\cdot C_b & \text{for} & t > t_{surf} \end{Bmatrix} \tag{19}$$

where C_b is described by one of the three bulk release mechanisms discussed above. In this work, we aimed to fit controlled release data with a variety of models and parameter combinations. Fitting was therefore conducted manually, with parameter values adjusted until a good fit was obtained. These data fitting methods are further elaborated upon in the discussion section.

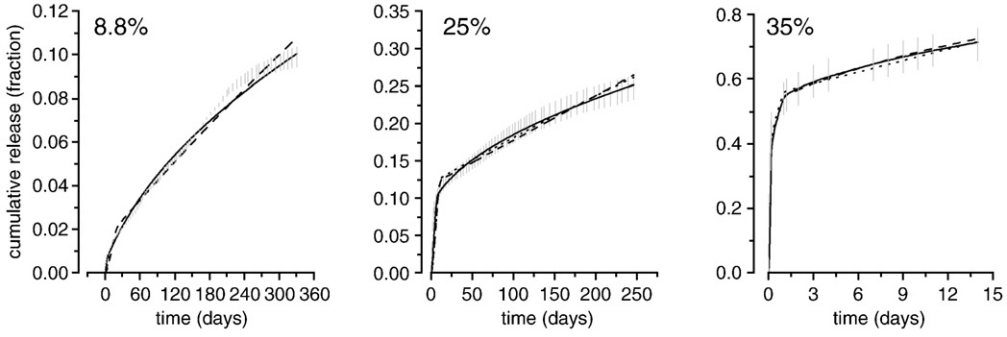

Diffusion Surface Dissolution				Diffusion Surface Dissolution Bulk Dissolution					Osmotic Gradient Surface Dissolution			
ϕ fraction	D $m^2/s\cdot10^{20}$	ω $s^{-1}\cdot10^6$	ζ fraction	D $m^2/s\cdot10^{20}$	ω $s^{-1}\cdot106$	ζ fraction	k $m/s\cdot10^{17}$	C_{sat} fraction	C_0 fraction	t_b days	ω $s^{-1}\cdot10^6$	ζ fraction
0.088	5.2	6	0.005	0.5	1	0.015	3.5	0.054	1	45	1	0.015
0.25	2.2	3	0.09	0.1	2	0.12	18	0.054	1	72	2	0.118
0.35	110	80	0.5	20	80	0.52	1200	0.054	1	3	80	0.55

Fig. 3. Predicting the release PTx from SIBS with various controlled release models. Many parameter combinations could be shown to produce good data fits for 8.8, 25 and 35% loading of PTx in SIBS; only one example of each model is included here. Solid lines replicate the data fits from the figure that describe release due to Fickian diffusion and surface dissolution. Dashed lines indicate release predictions due to diffusion, surface dissolution and bulk dissolution. Dotted lines describe release of drug to the osmotic gradient mechanism and surface dissolution. Experimental error (standard deviation) for release measurements of 8.8 ($n=3$), 25 ($n=12$) and 35% ($n=4$) formulations is indicated by the grey, vertical lines.

3. Results

The rate of release of PTx from SIBS polymer was measured for three loading amounts of drug in polymer (8.8, which is the commercial TAXUS® Express® formulation, 25, and 35%, Fig. 2). Release profiles were observed to be biphasic for all loading amounts: an initially high rate of drug release was followed by a longer phase of slow release. The magnitude and duration of the initial release phase, as well as the rate of release in the second phase, were dependent on loading percentage. Greater loading of drug in polymer resulted in greater initial release and faster overall release. For each of the loadings, incomplete release of drug was observed during the time frame studied here.

Fig. 3 provides a summary of fits of the models to experimental data. Models describing Fickian diffusion alone did not fit the data well (data not shown). The addition of surface dissolution to Fickian diffusion yielded good fits for each of the loading percentages, with fitted diffusion coefficients on the order of 10^{-20}–10^{-18} m^2/s (the diffusion coefficients that we obtained from these data fits are low compared values calculated for release of PTx from a different polymer [31], however, the release profiles are similar in shape to other published work [32]). The improvement in data fits observed with the addition of a model describing surface dissolution was especially noticeable for high loading percentages of PTx in SIBS. However, even accounting for the high initial release rates, the steady-state release was characterized by an effective diffusion coefficient that varied significantly with drug loading in polymer: between 8.8 and 25%, the fitted diffusion coefficient decreased by a factor of 2; between 25 and 35%, the fitted diffusion coefficient increased by a factor of approximately 50.

AFM studies were conducted on the cut surface of the TAXUS® Express® stent. These studies suggest that PTx is not miscible with SIBS (Fig. 4), since drug (identifiable as light patches) was found to be concentrated in discrete particulate areas in the polymer coating (identifiable as dark regions). Our analysis confirms previous reports that PTx is not miscible within SIBS [4,24]. Since drug is located in discrete particulate areas, the rate of dissolution of drug into the polymer phase through the polymer coating thickness would be expected to influence release kinetics. To account for this bulk dissolution process, a source term was added to the differential equation describing Fickian diffusion. Qualitatively, incorporation of bulk and surface dissolution terms produced data fits that were similar to those incorporating surface dissolution alone (Fig. 3); quantitatively, the value of the diffusion coefficient was still observed to change significantly between 8.8 and 35% loading. Additionally, the governing transfer coefficient of PTx in SIBS was observed to change by a factor of 340 among the loading percentages. Increasing D or k increases the rate of release for the bulk dissolution model, and so it was possible to produce combinations of D and k values that were unrealistic (for example, $D = 1\times10^{-27}$ cm^2/s and $k = 5\times10^{-17}$ m/s for 8.8%, data fit not shown). Systematic variation of k, D, ζ or ω was attempted, but it was not possible to obtain good fits to the data while maintaining any of the critical parameters constant with loading.

The alternative mechanism of release tested here assumes that osmotic pressure drives water into channels formed through an impermeable polymer coating. Considering the low solubility of PTx in water, large osmotic gradients seem unlikely; however, this model of drug release should still apply if finite solubility of PTx in water and lower solubility of water in the polymer coating is assumed, which does seem relevant in this system. The osmotic gradient model contains two parameters of interest: t_b, the time for a capsule to burst, and x, the distance between particle centers. Whereas x is an explicit function of the drug loading in polymer (given by Eq. (5)), t_b is indirectly related to particle size, since its value will depend on the osmotic gradient generated by the drug. Unlike Fickian diffusion, the parameters that characterize the osmotic gradient release mechanism

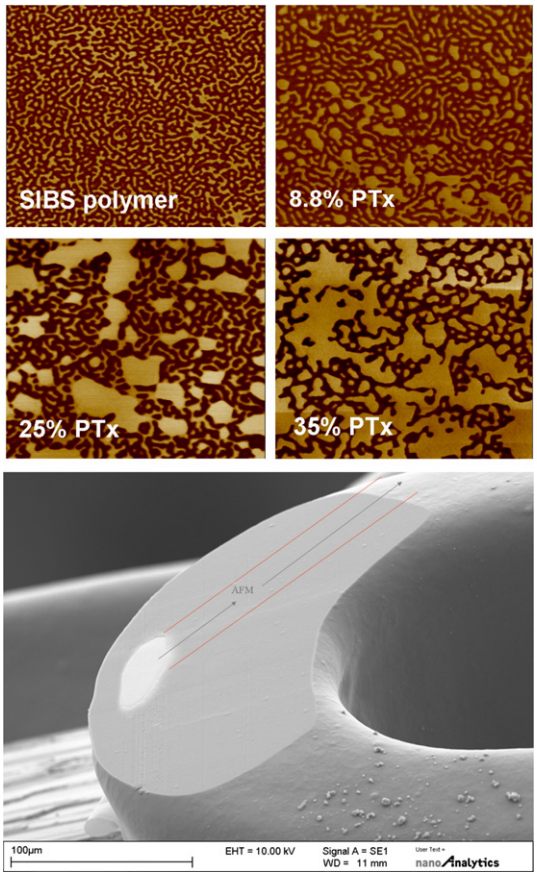

Fig. 4. AFM phase images (2 µm × 2 µm) of subsurface stent coatings showing morphology of SIBS polymer without drug and with paclitaxel incorporated at 8.8, 25 or 35% loading of drug in polymer [2]. Images highlight the two-phase morphology of the polymer as well as the distribution and increasing size of drug depots (large light colored spaces) as percent drug loading increases. The SEM (lower panel) shows a typical coated stent after cryomicrotomy preparation of subsurface samples for AFM.

are closely related to the assumed particle size and are expected to change with loading of drug in polymer.

The osmotic gradient model predicts constant release over time for slab geometry and near constant release for cylinders with a large radius of curvature; therefore, accounting for release via the osmotic gradient mechanism alone did not yield accurate fits to the data. As observed for Fickian diffusion model, incorporation of a surface dissolution yielded excellent data fits, particularly for high loadings of drug in polymer. An increase in loading from 8.8 to 25% resulted in a greater value for t_b (i.e., larger particles of drug amounted to slower bursting of each particle), however, the fitted value of t_b decreased for 35% loading of drug in polymer (i.e., larger particles of drug amounted to faster bursting of each particle). The discontinuity observed in the fitted value for t_b is similar to the discontinuity observed in the fitted value for D.

An interesting result of this analysis is that the data fits obtained for Fickian diffusion with surface dissolution and/or bulk dissolution were similar in quality to the data fits obtained with the osmotic gradient model with surface dissolution. The Fickian diffusion fit was characterized by some curvature throughout drug release, whereas the osmotic gradient model is almost entirely linear until the very last stages of release; this final stage was not achieved in any of our release measurements. Although the early curvature of the Fickian diffusion model could be argued to be a more accurate depiction of the data, this benefit disappeared at higher loadings of drug in polymer. Any data-fitting benefit of early curvature due to the specific bulk release mechanism was overwhelmed by the benefit of a surface dissolution term.

Table 2
Summary of known, unknown and fitted parameters utilized in this work.

	Parameter	Value	Source	Factor
Known	L, coating half-thickness	$1.4–5.7\times10^{-6}$ m	Theoretical, based on coating weights	N/A
	ρ, density	1000 kg/m^3	Assumed, density of water	N/A
	φ, drug loading	0.088,0.25, or 0.35 v/v	Known	N/A
	R_{cyl}, cylindrical radius	$1.4–5.7\times10^{-6}$ m	Equal to the half-thickness	N/A
Unknown	C_s, solubility of drug in media	0.03 kg/m^3	Calculated from solubility tests	Media conditions: temperature, fluid flow, osmotic pressure
	R, drug particle radius	$3.6–11\times10^{-8}$ m	Extrapolated from AFM data	Formulation parameters: solvent and spray conditions
	C_p, solubility of drug in polymer	0.054 v/v	Calculated from solubility tests	Drug-polymer interactions
	x, average distance between drug particle centers	$0.3–4\times10^{-4}$ m	Calculated from Eq. (5)	Formulation parameters and drug properties
Fitted[a]	D_{eff}, effective diffusion coefficient	10^{-21}–10^{-17} m^2/s	Fitted to experimental data	Function of molecular weight: affected by pore size and drug-polymer interactions
	ω, surface dissolution parameter	10^{-7}–10^{-5} s^{-1}	Chosen to obtain observed time to completion of surface dissolution	Media conditions: temperature, fluid flow, osmotic pressure
	ζ, fraction of drug available for surface dissolution	0–0.60 v/v	Chosen to obtain observed magnitude of surface dissolution	Formulation parameters, uniformity of coating, drug particle radius
	k, mass transfer coefficient from drug to polymer	10^{-18}–10^{-14} m/s	Fitted to experimental data	Drug-polymer interactions
	h, mass transfer coefficient from drug to media	10^{-4}–1 m/s	Fitted to experimental data	Drug-media interactions
	t_b, time for a drug capsule to burst	10^5–10^7 s	Fitted to experimental data	Osmotic pressure and mechanical properties of the polymer

[a] Since many parameter combinations were possible and not all of the plausible data fits are shown, the possible parameter listed here cover a greater range than the samples provided in Fig. 3.

The effect of surface dissolution depends on choice of ζ and ω, where ω is directly related to the ratio of the convective transfer coefficient (h), solubility of PTx in solution (C_s), PTx density (ρ), and particle radius (R), as described in Eq. (17). Choice of these parameters influences ω, which, in turn, determines the time to completion of surface dissolution. For example, an increase in the convective transport coefficient would increase the rate of surface dissolution and would increase the value of ω. A summary of the parameter estimates chosen for this work is provided in Table 2. Within a range of reasonable values, the exact value of many parameters is not known. It is evident that there is a combined uncertainty in some of the critical parameter values of at least one order of magnitude. We therefore observe an important feature of this modeling experiment: a model that incorporates more parameters may appear to improve a data fit, however, with each additional (uncertain) parameter, the confidence in the fit is reduced.

The percentage of particles that touch the surface, ζ, determines the fraction of release originating from the surface particles and has the most significant effect on the overall goodness of fit. Coherent anti-stokes Raman scattering (CARS) microscopy ([23]) suggest that drug dispersion is uniform throughout the polymer coating, and this uniformity of drug dispersion is further supported by AFM studies of bulk coating cross sections Ranade et al., [4]. If drug is uniformly distributed and assumed to be contained within spherical drug regions, then ζ should be given by the ratio of particle radius to coating thickness. However, as seen on the images of coating cross-sections in Fig. 4, the drug domains are not typically spherical. Furthermore, the two-dimensional images do not capture the three dimensional shape of these domains, which increase in size and asymmetry as drug loading increases. AFM therefore does not capture the drug depot size differences that lie just below the surface. R was measured from AFM data (Fig. 4), and the fraction of release due to surface dissolution would be estimated at 0.002, 0.03, and 0.04 based on the assumption of uniformly distributed spherical particles (Table 3), yet it is clear from the controlled release data (Fig. 2) that surface release fractions are more likely to be larger than this, on the order of 0.005–0.015, 0.09–0.15, and 0.45–0.55. In the face of the significant discrepancy between predicted and fitted particle radius values, it must be recognized that even though the addition of a surface release model fits the data well, it does not capture the physics underlying release. It is possible that variation in sub-surface morphology at different loadings could produce variation in the degree of interconnectedness between drug polymers. Since interconnected pores would be expected to result in faster release, percolation effects complicate the interpretation of these parameter values. For example, at the highest loading percentage, we would expect that surface release would be least influential, since the interconnectedness of the pores would lessen the difference between surface-associated and bulk-polymer-associated particles of drug. Instead, the highest loaded stent is characterized by the greatest difference between fast, early release (presumably representative of surface-associated drug), and slow, later release (presumably representative of bulk-polymer-associated drug). There may also be indirect effects of the release media that are not explicitly included in the model. Even if it were possible to know the exact pore structure within polymer and the effects of media on release behavior, there are no mathematical models available to account for the release behavior that we observe.

Table 3
Predicted and fitted surface release fraction.

Loading (fraction)	Coating thickness (μm)	Particle radius (nm)	Predicted ζ (fraction)	Fitted ζ (fraction)
0.088	11.4	36	0.003	0.005–0.015
0.25	3.8	70	0.02	0.09–0.11
0.35	2.9	110	0.04	0.45–0.55

4. Discussion

A model with high predictive value may be an important contribution to understanding how the output of a system will change with time, or how *in vitro* data may be interpreted in the context of *in vivo* application. Investigators often apply mathematical models to the controlled release of drugs from polymeric stent coatings [7,25–29], yet none of these current studies provide a convincing link between the kinetics of release and the underlying physical mechanism.

To test the value of a model rigorously, the majority of parameters described within the model should be known; perhaps one or two parameters would be fit to a particular application. The models described here do not meet this criterion, which is common for models of controlled release. Our observations suggest an important feature of any attempt to predict controlled release phenomenon with mechanistic models: the goodness of fit of the model is not, on its own, an accurate way to justify a physical mechanism. For example, other 'zero-order' release models are available for evaluation, all of which depend on different release mechanisms, including swelling [15], dissolution [30], or non-uniform drug loading [13]. The ability of each model to predict a near constant rate of release for periods of time is based on a different set of assumptions, parameter values and degrees of freedom in the data fit. Decisions regarding mechanisms of controlled release could be gained from models that are tested in ways other than their fit effectiveness, particularly if measurements are made under more than one experimental condition. One useful way to test a model is to evaluate which features are fixed, or known in value, and which features of the model can be altered experimentally. By systematically varying experimental parameters and comparing their effect to the predicted output, evidence could be accumulated that either supports or calls into question the basic physical principles suggested by the model.

In this work, several models that account for drug release by different mechanisms were applied to data from controlled release measurements. It is clear from these experiments that while both the Fickian diffusion and osmotic gradient models accurately predict the rate of drug release, neither model provides a satisfying account of the mechanisms of drug release. Release via Fickian diffusion would be expected to occur as drug migrates through the polymer matrix, yet PTx is not miscible in SIBS; PTx is not expected to diffuse through polymer. Drug release via an osmotic gradient mechanism would be expected to occur when drug has high osmotic activity, yet PTx is poorly soluble in water and SIBS is impermeable to water; the osmotic gradient for PTx is not expected to be large. The most dramatic improvement to data fitting was obtained by accounting for the initial high rate of release with a model of surface dissolution. However, the observed fractions of initial drug release (0–0.55) are inconsistent with prior characterization of PTx/SIBS that demonstrated uniform loading of drug in polymer, suggesting that surface dissolution does not provide a complete account for the mechanism of initial drug release either. Finally, key parameter values (D, h, k, ω) would be expected to remain constant for different loadings of drug in polymer; the variation of these fitted parameters across several orders of magnitude calls the value of determining model mechanisms by data fitting into further question.

Our comparison of mathematical models suggests several features of drug release. First, models that accounted for release via different physical mechanisms were able to fit the data well. Second, within predictions from any given model, multiple parameter combinations were capable of producing fits of nearly equivalent quality. Third, it was not possible to obtain adequate fits to the data by holding any of the critical model parameters constant between loading percentages. Fourth, not all of the model parameters could be known with great certainty.

In a typical study, data fitting would proceed via regression analysis. We have two concerns with this approach. First, controlled release data are non-uniformly distributed. In general, more data points are collected at early stages of release than at later stages of release. Second, these data are correlated, and a greater number of data points do not necessarily indicate greater importance of those values. Regression analysis serves to minimize the sum of square error; this process will yield an unbiased fit to the *available* data, but the parameter estimates of the underlying function will be highly influenced (and potentially biased) by the frequency and spacing of data collection. The non-uniform spacing and correlated nature of controlled release data violate the assumptions of regression analysis, and therefore reduce the ability of regression analysis to be used in a predictive capacity. This analytical dilemma is compounded when the chosen model does not fit the shape of the data well, since the non-uniform distribution of data will arbitrarily emphasize aspects of the model that might not be mechanistically relevant. Techniques are available to correct for the problems of non-uniform spacing and correlated data [33,34], however, these methods are not well-established and require mathematical rigor that is generally beyond the scope of a controlled release experiment. It would also be possible to expand on the basic data fitting technique through comparison of model fitting utility with standard statistical techniques (e.g., Akaike's Information Criterion or Schwarz Criterion). However, we argue that such quantitative analysis would only serve to further mislead a researcher into choosing a data fit that is statistically "best" but mechanistically poor.

The usefulness of data fitting depends on the intended purpose of the experiment. We propose that the purpose of modeling controlled release data be critically examined prior to data fitting experiments. Data fits obtained from solutions to well-established governing equations such as Fick's Law are useful for the estimation of standard parameter values (e.g., the diffusion coefficient) which are easily comparable between experiments. The consistent use of a standard model allows for straightforward comparison of release profiles obtained in different experiments, and the utility of this feature should not be underestimated.

A model that provides accurate data fits could be useful for release rate prediction. For example, in Fig. 5a, the rate of release of PTx from 25 and 35% loaded stents was predicted for time points that were not experimentally measured. Extrapolations generated by diffusion with surface dissolution or the osmotic gradient with surface dissolution produced similarly shaped curves, however, the magnitude of release varied significantly between the two predictive models. Therefore, data should not be extrapolated from a modeling prediction unless the release mechanism is certain.

Perhaps most importantly, a model that contains only one or two parameter values could allow for interpolation of fitted parameter values to theoretical conditions not measured. For example, the value of the diffusion coefficient can be predicted for varying temperatures (the experimental validity of this method has been demonstrated repeatedly for instances where the transport mechanism is known to be diffusive). Linear parameter interpolation was attempted in Fig. 5b in order to predict the rate of release of PTx from a theoretical, 30% loaded stent, but the predictions generated by the Fickian model and the osmotic gradient were significantly different. It is not possible to

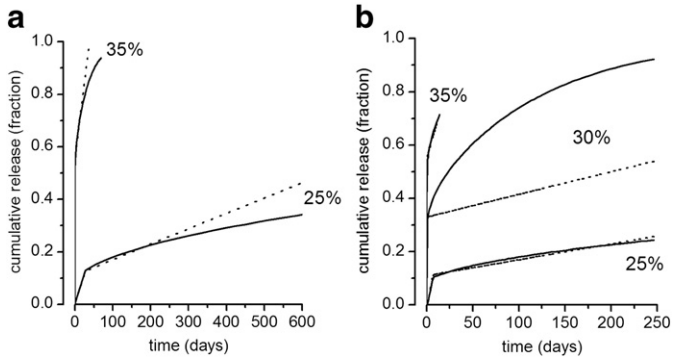

Fig. 5. Predicting unknown data by the diffusion and osmotic gradient models. Solid lines describe release due to Fickian diffusion and surface dissolution. Dotted lines describe release of drug to the osmotic gradient mechanism and surface dissolution. (a) Model predictions were extrapolated to cover time periods not observed in this experiment. (b) D, t_b, ω and ζ were linearly interpolated from data fits of 25 and 35% loadings to produce predictions of controlled release for a theoretical, 30% loaded stent. The parameter values utilized for 25% and 35% loading are described in Fig. 3.

develop a reliable extrapolation method without extensive experimental validation, and so the application of a complex, unverified model is limited. Therefore, even if a model has high predictive value, a mechanism of release must be certain in order to predict controlled release rates that are not experimentally measured.

The modeling processes described in this work are similar to modeling results published elsewhere. A less thorough analysis (for example, if only two loading percentages were studied) would not have revealed the model flaws discussed here. Furthermore, the accuracy of data fitting is severely limited by the use of models that rely on more than one (uncertain) parameter value. We conclude that better information on the physics of drug incorporation into, and diffusion through, polymer materials is needed for progress in mathematical modeling of novel controlled release systems.

5. Conclusions

The theoretical predictions of several mechanistic models were compared to experimental measurements of the release of PTx from a SIBS polymer matrix affixed to stents. Experimentally, higher loading of drug in polymer resulted in a greater amount of initial drug release and an overall faster rate of release. Although it was possible to accurately fit the in vitro data with models accounting for drug release by different mechanisms, it was also evident that the physics of release were not fully captured by any of the models studied here. These results demonstrate the complexity of drug release in the real world, and show that models, of themselves, cannot substitute for experimental data. Therefore, for the more general case of the application of mechanistic models of drug release, data fitting should proceed with caution. Data fits obtained from models containing more than one parameter could be misleading. Even if the model fits well, the results cannot necessarily be applied to circumstances beyond what was experimentally measured. Greater certainty in parameter values, the measurement of release under varying conditions, the comparison of multiple models, and determination of intended model use prior to model application would improve the utility of data fitting experiments. We therefore conclude that when the mechanism of drug release is not known, the simplest model with good predictive value is desired.

Acknowledgements

The authors wish to thank Dr. Shrirang Ranade (formerly of BSC) and Dr. Michael Allen (BIOMETROLOGY, Inc.) for AFM support. We also thank the anonymous reviewers, for providing helpful critique that significantly improved the presentation of this work.

References

[1] C. Herdeg, M. Oberhoff, K.R. Karsch, Antiproliferative stent coatings: taxol and related compounds, Semin. Interv. Cardiol. 3 (1998) 197–199.
[2] K.R. Kamath, J.J. Barry, K.M. Miller, The taxus drug-eluting stent: a new paradigm in controlled drug delivery, Adv. Drug Delivery Rev. 58 (2006) 412–436.
[3] G.W. Stone, S.G. Ellis, L. Cannon, J.T. Mann, J.D. Greenberg, D. Spriggs, C.D. O'Shaughnessy, S. DeMaio, P. Hall, J.J. Popma, J. Koglin, M.E. Russell, Comparison of a polymer-based paclitaxel-eluting stent with a bare metal stent in patients with complex coronary artery disease: a randomized controlled trial, J. Am. Med. Assoc. 294 (2005) 1215–1223.
[4] S.V. Ranade, K.M. Miller, R.E. Richard, A.K. Chan, M.J. Allen, M.N. Helmus, Physical characterization of controlled release of paclitaxel from the taxus express drug-eluting stent, J. Biomed. Mater. Res., Part A. 71 (2004) 625–634.
[5] J.-Z. Chen, S.V. Ranade, X.-Q. Xie, NMR characterization of paclitaxel/poly (styrene–isobutylene–styrene) formulations, Int. J. Pharm. 305 (2005) 129–144.
[6] T. Higuchi, Mechanism of sustained-action medication. Theoretical analysis of rate of release of solid drugs dispersed in solid matrices, J. Pharm. Sci. 52 (1963) 1145–1149.
[7] P. Costa, J.M. Sousa Lobo, Modeling and comparison of dissolution profiles, European J. Pharm. Sci. 13 (2001) 123–133.
[8] P.L. Ritger, N.A. Peppas, A simple equation for desciption of solute release I. Fickian and non-Fickian release from non-swellable devices in the form of slabs, spheres, cylinders or discs, J. Control. Release 5 (1987) 23–36.
[9] J. Siepmann, H. Kranz, R. Bodmeier, N.A. Peppas, HPMC-matrices for controlled drug delivery: a new model combining diffusion, swelling, and dissolution mechanisms and predicting the release kinetics, Pharm. Res. 16 (1999) 1748–1756.
[10] R.S. Harland, A. Gazzaniga, M.E. Sangalli, P. Colombo, N.A. Peppas, Drug/polymer matrix swelling and dissolution, Pharm. Res. 5 (1988) 488–494.
[11] N.A. Peppas, Analysis of fickian and non-fickian drug release from polymers, Pharm. Acta Helv. 60 (1985) 110–111.
[12] X. Huang, C.S. Brazel, On the importance and mechanisms of burst release in matrix-controlled drug delivery systems, J. Control. Release 73 (2001) 121–136.
[13] P.I. Lee, Novel approach to zero-order drug delivery via immobilized nonuniform drug distribution in glassy hydrogels, J. Pharm. Sci. 73 (1984) 1344–1347.
[14] H. Leuenberger, J.D. Bonny, M. Kolb, Percolation effects in matrix-type controlled drug release systems, Int. J. Pharm. 115 (1995) 217–224.
[15] K.G. Papadokostaki, A.Y. Polishchuk, J.K. Petrou, Modeling of solute release from polymeric monoliths subject to linear structural relaxation, J. Polym. Sci., Part B: Polym. Phys. 40 (2002) 1171–1188.
[16] B. Amsden, A model for osmotic pressure driven release from cylindrical rubbery polymer matrices, J. Control. Release 93 (2003) 249–258.
[17] M.V.S. Varma, A.M. Kaushal, A. Garg, S. Garg, Factors affecting mechanism and kinetics of drug release from matrix-based oral controlled drug delivery systems, Am. J. Drug Delivery 2 (2004) 43–57.
[18] S. Prabhu, S. Hossainy, Modeling of degradation and drug release from a biodegradable stent coating, J. Biomed. Mater. Res., Part A 80 (2007) 732–741.
[19] V. Dua, Controlled release of drugs from polymeric devices, Comp. Aided Chem. Eng. 24 (2007) 971–976.
[20] M.J. Abdekhodaie, X.Y. Wu, Drug release from ion-exchange microspheres: mathematical modeling and experimental verification, Biomaterials 29 (2008) 1654–1663.
[21] W.D. Lindner, J.E. Mockel, B.C. Lippold, Controlled release of drugs from hydrocolloid embeddings, Pharmazie 51 (1996) 263–272.
[22] G. Csoka, J. Dredan, S. Marton, I. Antal, I. Racz, Evaluation of different mathematical methods describing drug liberation from new,'soft-patch' type matrix systems, Pharm. Dev. Technol. 4 (1999) 291–294.
[23] L. Zhang, C. Long, J. Pan, Y. Qian, A dissolution-diffusion model and quantitative analysis of drug controlled release from biodegradable polymer microspheres, Can. J. Chem. Eng. 84 (2006) 558–566.
[24] E. Kang, H. Wang, I.K. Kwon, Y.H. Song, K. Kamath, K.M. Miller, J. Barry, J.X. Cheng, K. Park, Application of coherent anti-stokes raman scattering microscopy to image the changes in a paclitaxel-poly(styrene-b-isobutylene-b-styrene) matrix pre- and post-drug elution, J. Biomed. Mater. Res., Part A 87 (2008) 913–920.
[25] D.V. Sakharov, L.V. Kalachev, D.C. Rijken, Numerical simulation of local pharmacokinetics of a drug after intravascular delivery with an eluting stent, J. Drug Targeting 10 (2002) 507–513.
[26] C.W. Hwang, D. Wu, E.R. Edelman, Impact of transport and drug properties on the local pharmacology of drug-eluting stents, Int. J. Cardiovasc. Intervent. 5 (2003) 7–12.
[27] P. Zunino, Multidimensional pharmacokinetic models applied to the design of drug-eluting stents, Cardiovasc. Eng. 4 (2004) 181–191.
[28] B.S.B. Balakrishnan, A.R.P. Tzafriri, P.M.S. Seifert, A.M.S. Groothuis, C.M.D. Rogers, E.R.M.D.P. Edelman, Strut position, blood flow, and drug deposition: implications for single and overlapping drug-eluting stents, Circulation 111 (2005) 2958–2965.
[29] C. Yang, H.M. Burt, Drug-eluting stents: factors governing local pharmacokinetics, Adv. Drug Delivery Rev. 58 (2006) 402–411.
[30] G. Frenning, Theoretical investigation of drug release from planar matrix systems: effects of a finite dissolution rate, J. Control. Release 92 (2003) 331–339.
[31] F. Alexis, S. S. Venkatraman, S. K. Rath, F. Boey, In vitro study of release mechanisms of paclitaxel and rapamycin from drug-incorporated biodegradable stent matrices, J. Control Release 98 (2004) 67–74.
[32] L. Fung, M.G. Ewend, A. Sills, E.P. Sipos, R. Thompson, M. Watts, O.M. Colvin, H. Brem, W.M. Saltzman, Pharmacokinetics of interstitial delivery of carmustine, 4-hydroperoxycyclophosphamide, and paclitaxel from a biodegradable polymer implant in the monkey brain, Cancer Res. 58 (1998) 672–684.
[33] W. Dunsmuir, P.M. Robinson, Estimation of time-series models in the presence of missing data, J. Am. Stat. Assoc. 76 (1981) 560–568.
[34] H. Garnier, L. Wang, Identification of continuous models from sampled data, first ed. Springer, New York, 2008.